

Photocatalytic decomposition of benzene with plasma sprayed TiO₂-based coatings on foamed aluminum

Huang Chen^{a,*}, Soo Wahn Lee^a, Tae Ho Kim^a, Bo Young Hur^b

^a Interface Engineering Laboratory, Department of Materials Engineering, Sun Moon University, Asan, ChungNam 336708, South Korea

^b Department of Materials Engineering, Gyeong Sang National University, ChinJu 660701, South Korea

Received 24 September 2004; received in revised form 20 April 2005; accepted 29 April 2005

Available online 13 June 2005

Abstract

Plasma spraying technique was used to deposit thin TiO₂-based photocatalytic coatings on foamed aluminum. Before plasma spraying, the composites of nano-TiO₂ powder (P25) and nano-ZnO/CeO₂/SnO₂ powders were agglomerated into microsized powders by spray-drying process. X-ray diffraction (XRD), Scanning electron microscopy (SEM), Transmission electron microscopy (TEM), X-ray photoelectron spectroscopy (XPS) and photocatalytic activity evaluation by the decomposition of gas-phase benzene (C₆H₆) were applied to characterize the starting powders and the coatings, respectively. The results showed that all the three plasma sprayed TiO₂-based coatings were the mixture phases of anatase and rutile. On the splats' surfaces of the as-sprayed coatings, fine nano-crystalline particles were observed. However, grain growth occurred on the surface of plasma sprayed 90%TiO₂–10%ZnO coating. The XPS spectra revealed that the Ti, Zn, Ce and Sn elements existed on the surfaces of plasma sprayed TiO₂-based coatings as the chemical states of Ti⁴⁺, Zn²⁺, Ce⁴⁺ and Sn⁴⁺, respectively, whilst, the oxygen element was composed of three kinds of chemical states, i.e. crystal lattice oxygen, hydroxyl oxygen and physical-adsorbed oxygen. It was found that plasma sprayed 90%TiO₂–10%CeO₂ coating and 90%TiO₂–10%SnO₂ coating exhibited similar photocatalytic activity, which was higher than that of plasma sprayed 90%TiO₂–10%ZnO coating. The photocatalytic activity is not only dependent on the anatase content but also on the surface morphology and the hydroxyl content formed on the surface of plasma sprayed TiO₂-based coatings as well as the additive character.

© 2005 Elsevier Ltd. All rights reserved.

Keywords: Plasma spraying; TiO₂; Benzene; Photocatalyst; Coatings

1. Introduction

Titanium dioxide (TiO₂) has been extensively applied in paints and pigments as a whitening agent due to its good scattering effect against ultraviolet. Since Fujishima and his co-workers¹ first discovered the photooxidation of water by TiO₂ electrodes in 1972, a large number of applications of TiO₂ material in photocatalytic technology have been developed, such as self-cleaning, air cleaning, water purification, anti-tumor and self-sterilizing.² When exposed to UV light, TiO₂ can decompose various organic contaminants into non-

toxic compounds like water and CO₂. However, its photocatalytic activity still needs to be enhanced in particular for water purification. In the past two decades, several methods were adopted to improve the photocatalytic activity of TiO₂, such as increasing the surface area by reducing grain size,^{3–7} doping noble metals⁸ or preparing composite photocatalyst.⁹

Usually, TiO₂ photocatalyst is utilized both in the forms of powder and coating/film. The powder-type TiO₂ photocatalyst has more effective resulting from its larger specific surface area than coating/film. But, due to some problems arising from practical application, such as dispersion of powder-type photocatalyst, separation of powder-type photocatalyst after the photocatalytic reaction as well as reusing of powder-type photocatalyst, TiO₂ photocatalyst in the form of coating/film is preferred to pursue today.^{10,11}

* Corresponding author. Tel.: +82 41 530 2882/2364;
fax: +82 41 543 2798.

E-mail address: jx_chuang@yahoo.com (H. Chen).

In this study, combined with spray-drying process used for aggregation of the binary nano-powders, plasma spraying technique was used to deposit the three kinds of TiO_2 -based photocatalytic coatings. Their phase composition, morphology and surface chemical state of the as-sprayed coatings were characterized. Benzene is one of the hazardous compounds emitted from flue gases due to its serious carcinogenicity. Using the photocatalytic decomposition of gas-phase benzene as a reaction model, their photocatalytic activities of the three kinds of plasma sprayed TiO_2 -based coatings were evaluated comparably.

2. Experimental procedures

2.1. Preparation of plasma spraying powder

TiO_2 powder (P25, Degussa, Germany), a mixture of 70–80% anatase and 20–30% rutile with grain size in the range of 20–50 nm as shown in Fig. 1a, was used as the basic powder in this study. Stemming from the consideration of improving photocatalytic activity of TiO_2 coatings, 10 wt.% nanosized semiconductors (ZnO, CeO_2 and SnO_2 , NanoTeck, Japan) were added, respectively, to TiO_2 powder before aggregation. Fig. 1 shows the TEM micrographs of

TiO_2 , ZnO, CeO_2 and SnO_2 . It is clearly seen that ZnO particles show rod shape with 20–50 nm in width and 20–100 nm in length as shown in Fig. 1b. CeO_2 and SnO_2 particles are less than 10 nm as can be seen from Fig. 1c and d. Besides, few bigger particles about 30 nm were found also.

Three slurries for spray-drying were made by the medium of distilled-water and milled for 24 h in a polyethylene jar with zirconia ceramic balls. In order to reduce the viscosity of slurry and increase the bonding strength of final aggregated powders, commercial dispersant polymethacrylic acid (PMAA, M_w : 9500, Sigma–Aldrich, USA) and binder polyvinyl alcohol (PVA, M_w : 124.00–186.00, Sigma–Aldrich, USA) were added, respectively. Then, the milled slurries were spray-dried by the machine (EYELA SD-1000, Tokyo Rikakikai Co., Ltd., Japan). The main controlled spraying conditions are tabulated in Table 1. In this study, the spraying conditions were fixed for the three kinds of slurries. A special attention was paid to their shape, powder size and productivity of the as-received powders.

2.2. Plasma spraying

The Metco A-2000 atmospheric plasma spraying equipment (F4-MB gun, Sulzer Metco AG, Switzerland) was

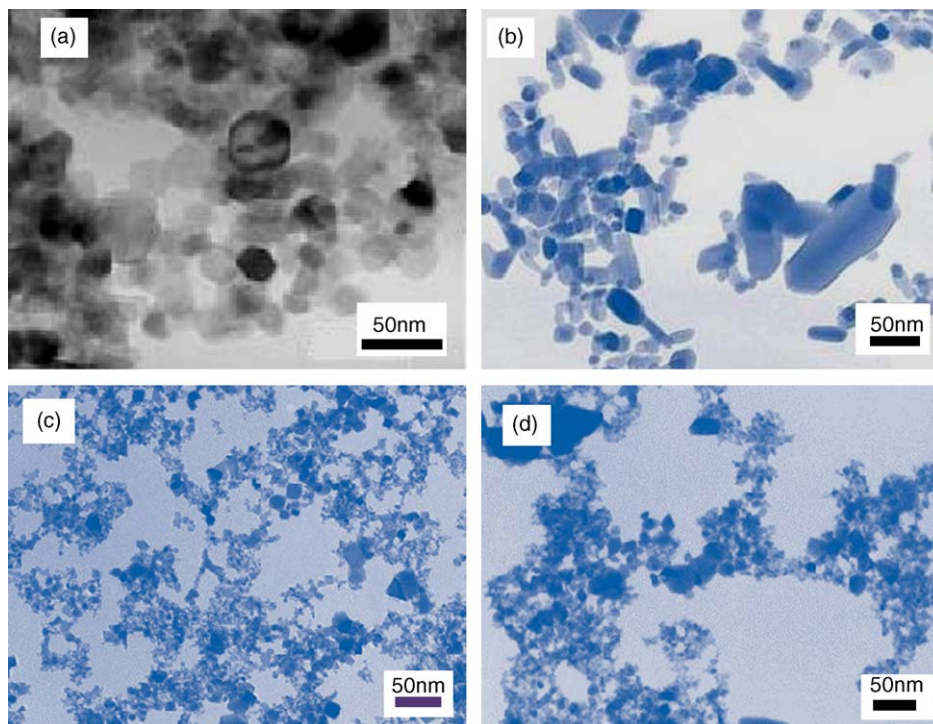


Fig. 1. TEM micrographs of the starting nano-particles: (a) TiO_2 , (b) ZnO, (c) CeO_2 and (d) SnO_2 .

Table 1
The spray-drying conditions

Conditions	Atomizing ($\times 10$ kPa)	Pump-speed (ml^3/h)	Blower (m^3/min)	Inlet/outlet temperature ($^\circ\text{C}$)
Value	14	65	0.24	155/72–80

Table 2
Plasma spraying parameters for the photocatalytic TiO₂-based coatings

Argon flow rate (slpm)	40
Hydrogen flow rate (slpm)	9
Carrier gas flow rate (slpm)	3.5
Spraying power (kW)	36.9
Spraying distance (mm)	150
Powder injector diameter (mm)	2.0
Torch traverse speed (mm/s)	9.6

used to deposit the photocatalytic TiO₂-based coatings with the as-received three kinds of spray-dried powders. The feedstock was fed with a Twin-system 10-V (Plasma-technik AG, Switzerland). Table 2 lists the plasma spraying parameters used in this study. To increase contact area with pollutant, foamed aluminum plate with dimensions of $30 \times 20 \times 1 \text{ cm}^3$ was used as the substrate. Fig. 2 shows the photograph of this kind of substrate, which possesses varied size pores with 2–8 mm in diameter. Double of the largest faces of the foamed substrates were deposited TiO₂-based coatings.

2.3. Characterization

An X-ray diffractometer (Rigaku, Tokyo, Japan) operating with Cu K α ($\lambda = 1.54056 \text{ \AA}$) radiation was applied to identify the phase compositions of the starting powders and the as-sprayed TiO₂-based coatings. Morphologies of the starting powders and the as-sprayed coatings were characterized with a JEM-200CX Transmission Electron Microscopy (Jeol, Tokyo, Japan) and a JSM-6700F Field Emission Scanning Electron Microscope (Shimadzu, Tokyo, Japan). For avoiding the disturbance of gold grains which are usually coated on sample's surface before SEM observation on the morphology of plasma sprayed TiO₂-based coatings, this step was omitted in this study. Surface chemical states of the three kinds of plasma sprayed TiO₂-based coatings were studied using X-ray photoelectron spectroscopy (ESCALAB 220-IXL). The XPS Mg K α provides non-monochromatic X-rays at 1253.6 eV.

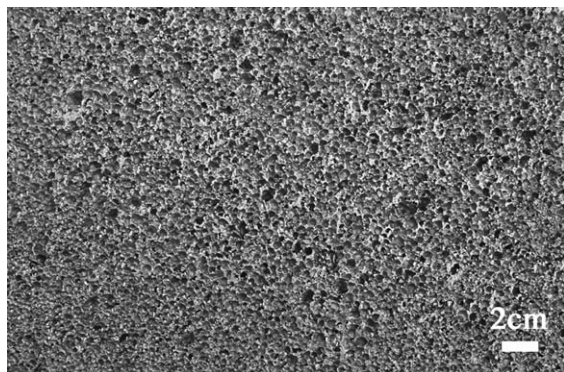


Fig. 2. Photograph of foamed aluminum substrate.

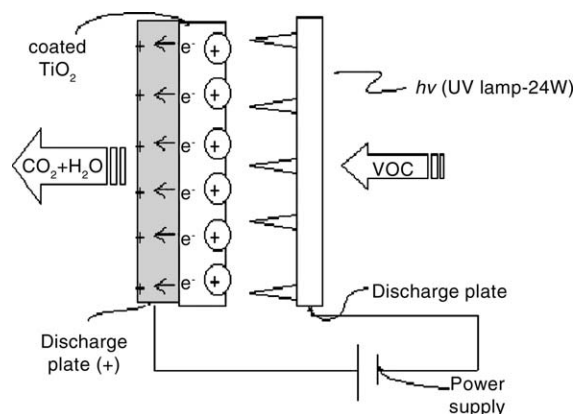


Fig. 3. Discharge photoelectron catalytic system.

2.4. Photocatalytic system

The discharge photoelectron catalytic system as shown in Fig. 3 was developed for increasing the photocatalytic activity by trapping electrons generated in photocatalyst upon UV irradiation and hence retarding electron–hole recombination. In this system, the foamed aluminum plates coated TiO₂-based coatings acted as the cathode and an array of copper strips in the shape of saw tooth was used as the anode. High voltage DC bias was used for the discharge. Five UV lamps (386 nm, 24 W, NEC Co., Japan) provided the photoexcitation source for the plasma sprayed TiO₂-based coatings. The photocatalytic activities of the three kinds of plasma sprayed TiO₂-based coatings deposited on the foamed aluminum plates were carried out comparably in a reactor of volume 1 m³, in which gas-phase benzene was injected by gastight syringes to prepare 100 ppm starting concentration. The changes of benzene concentration with irradiation time were measured at 30 min interval by a Gas Chromatography (HP-6890) equipped with a flame ionization detector (FID) and a capillary column (HP-5). Meanwhile, a blank test, the foamed aluminum plate without coating, was performed for comparison.

3. Results and discussion

3.1. Spray-dried powder characterization

3.1.1. Phase composition

Fig. 4 shows the XRD spectra of the three as-received powders aggregated by spray-drying process. It is noted that (1 0 1) peak at about $2\theta = 25.4^\circ$ of anatase phase is still the strongest peak for all the three kinds of powders, suggesting that all the as-received powders are mainly composed of anatase phase. The anatase contents in the three spray-dried powders were estimated from the XRD intensities of the anatase peak (1 0 1) at about $2\theta = 25.4^\circ$ and the rutile peak (1 1 0) at about $2\theta = 27.5^\circ$. This is a generally accepted method to evaluate anatase content in TiO₂ materials. The

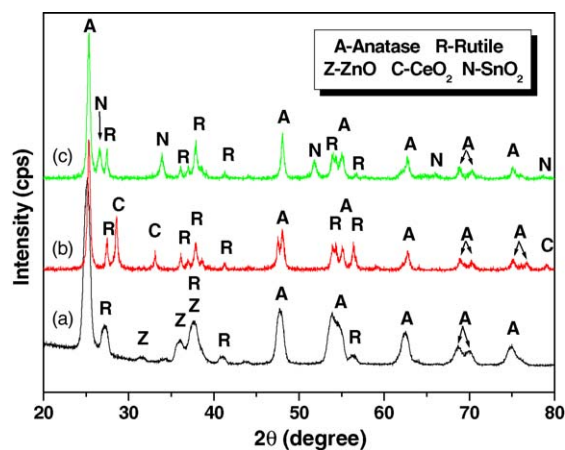


Fig. 4. XRD spectra of the spray-dried TiO_2 -based powders: (a) 90% TiO_2 –10% ZnO ; (b) 90% TiO_2 –10% CeO_2 ; and (c) 90% TiO_2 –10% SnO_2 .

estimated results are listed in Table 3. Their anatase contents are in the range of 75–79%, which is good agreement with the typical phase compositions of P25 TiO_2 powder as mentioned above. These results can be expected, because the operating temperature of spray-drying process is less than 155 °C as given in Table 1. As we know, the anatase-rutile transformation usually occurs in the temperature range from 400 to 1200 °C, hence there wasn't such phase transformation during the spray-drying process.

3.1.2. Morphology

As shown in Fig. 5, the three spray-dried powders show spherical shape and dense microstructure, despite their surfaces are not very smooth. Under the investigated conditions, their diameters of the as-received powders are in the range of 1–12 μm . During the consequent plasma spraying experiment, the three spray-dried powders demonstrated good flowability, which is ascribed mainly to their spherical morphology, dense microstructure and narrow size distribution. Moreover, the order of productivity

Table 3
Characteristic comparisons of the as-received powders and the as-sprayed coatings

Sample	Spray-dried powder		Coating
	Productivity (%)	Anatase content (%)	Anatase content (%)
90% TiO_2 –10% ZnO	61.6	78.3	45.5
90% TiO_2 –10% CeO_2	78.0	75.9	50.7
90% TiO_2 –10% SnO_2	69.1	78.8	37.8

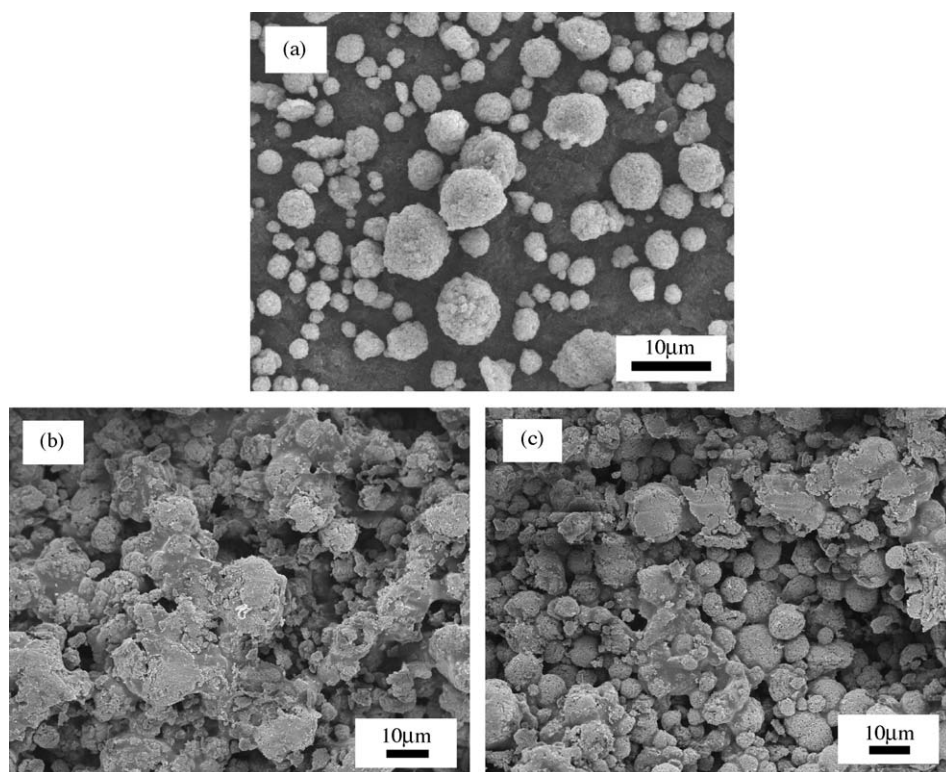


Fig. 5. SEM morphologies of the spray-dried powders: (a) 90% TiO_2 –10% ZnO , (b) 90% TiO_2 –10% CeO_2 and (c) 90% TiO_2 –10% SnO_2 .

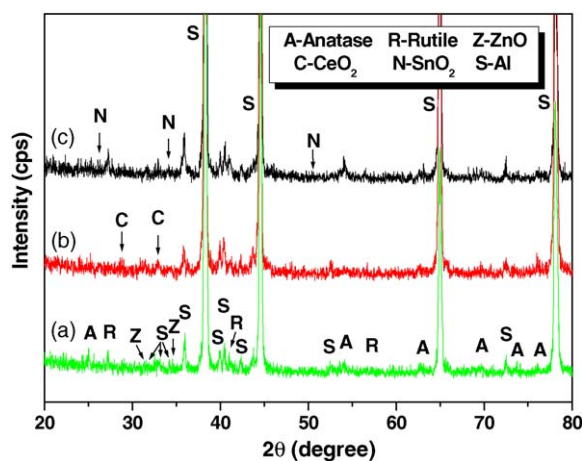


Fig. 6. XRD spectra of the plasma sprayed TiO_2 -based coatings deposited from the spray-dried powders: (a) 90% TiO_2 –10% ZnO ; (b) 90% TiO_2 –10% CeO_2 ; and (c) 90% TiO_2 –10% SnO_2 .

of the three kinds of spray-dried TiO_2 -based powders is 90% TiO_2 –10% CeO_2 > 90% TiO_2 –10% SnO_2 > 90% TiO_2 –10% ZnO . The exact values are listed in Table 3.

3.2. Coating characterization

3.2.1. Phase composition

The XRD spectra of the plasma sprayed TiO_2 -based coatings deposited from the three kinds of spray-dried powders are presented in Fig. 6. It is noticeable that the substrate (Al plate) displays several peaks with higher relative intensity resulting from their thin thickness of the plasma-sprayed TiO_2 -based coatings. In contrast, the peaks of TiO_2 are weak. Compared with the XRD spectra of those starting powders shown in Fig. 4, it was found that the anatase phase in the starting powders transformed partially to the stable rutile phase during the plasma spraying. Especially, for 90% TiO_2 –10% SnO_2 powder, its anatase content reduced remarkably from 78.8 to 37.8% in the as-sprayed coating as listed in Table 3. This phenomenon is inevitable, because the flame temperature of plasma spraying is extreme high temperature (>5000 °C). It is necessary to point out that plasma spraying technique possesses extreme cooling rate also, so some anatase phase were reserved in the plasma sprayed coatings. At the same time, high cooling rate is beneficial to form nanostructure in ceramic coatings. That is the reason why plasma spraying technique is often chosen to deposit nanostructured ceramic coatings recently.^{12,13} As can be seen from Table 3, the plasma sprayed 90% TiO_2 –10% CeO_2 coating has the highest anatase content (50.7%). In the case of plasma sprayed 90% TiO_2 –10% SnO_2 coating, it is only 37.8% which is the lowest among the three kinds of plasma sprayed TiO_2 -based coatings.

It seems that no chemical reaction occurred between TiO_2 and added ZnO , CeO_2 and SnO_2 during the plasma spraying, because there isn't any obvious peaks of their compositions

in the XRD spectra as shown in Fig. 6. This may be explained on the basis of quite short dwell time the powders experienced in the plasma flame. Another possible explanation is the considerable evaporation of ZnO , CeO_2 and SnO_2 during the plasma spraying when hydrogen was used as the auxiliary plasma gas.

3.2.2. Morphology

The plasma sprayed TiO_2 -based coatings are dark grey face and cover the largest two surfaces of the foamed aluminum plates. It is well known that photocatalytic reaction happens on the surface or in limited depth of photocatalyst. Thus, the surface morphology of photocatalyst is critical to its photocatalytic activity. In this study, the spray-dried TiO_2 -based powders were coated only one cycle on the surfaces of foamed aluminum plates. SEM observation on cross-section revealed that the coatings were bonded well to the substrates. However, the thickness is quite heterogeneous. The thickest section containing non-melted particles is up to 10 μm , while the thinnest region is only several hundred nanometers. All the mean thicknesses for the three kinds of plasma sprayed TiO_2 -based coatings are about 1–2 μm . Fig. 7 presents the typical FESEM surface morphologies of plasma sprayed TiO_2 -based coatings deposited from the three spray-dried powders under the same spraying parameters. These plasma sprayed coatings are characterized by rough surfaces with melted splats and non-melted or partially melted particles together. This structure is very porous, resulting in higher specific surface area. The melted splats have excellent flattening, while the non-melted or partially melted particles display ball-like shape resembling the starting nano-particle. Compared with the plasma-sprayed 90% TiO_2 –10% CeO_2 coating and the plasma sprayed 90% TiO_2 –10% SnO_2 coating, many grains on the surface of plasma sprayed 90% TiO_2 –10% ZnO coating has grown up to 100 nm as can be seen from Fig. 7a and b. The plasma sprayed 90% TiO_2 –10% CeO_2 coating and the plasma-sprayed 90% TiO_2 –10% SnO_2 coating show similar surface morphologies. On the splats' surfaces of the as-sprayed coatings, fine nano-crystalline particles were observed.

3.2.3. XPS analysis

XPS is a highly sensitive technique of surface analysis and often used to testify the surface composition and chemical state of solid samples. In this study, photoelectron peaks for elements Ti, Zn, Ce, Sn, O and C were recorded. Among them, the C1s peak, at a binding energy of ~286.0 eV, was used as the reference to correct the shift in XPS spectra. Due to its similarity, the spectrum wasn't given out. Fig. 8 presents the XPS of Ti2p on the surfaces of the three plasma sprayed TiO_2 -based coatings. It was noted that all the Ti2p XPS peaks were sharp and strong, revealing that the Ti element mainly existed as the chemical state of Ti^{4+} . Moreover, the XPS Ti2p on the surface of plasma sprayed 90% TiO_2 –10% SnO_2 coating was split into two peaks. One new peak at about 450.8 eV appeared as can be

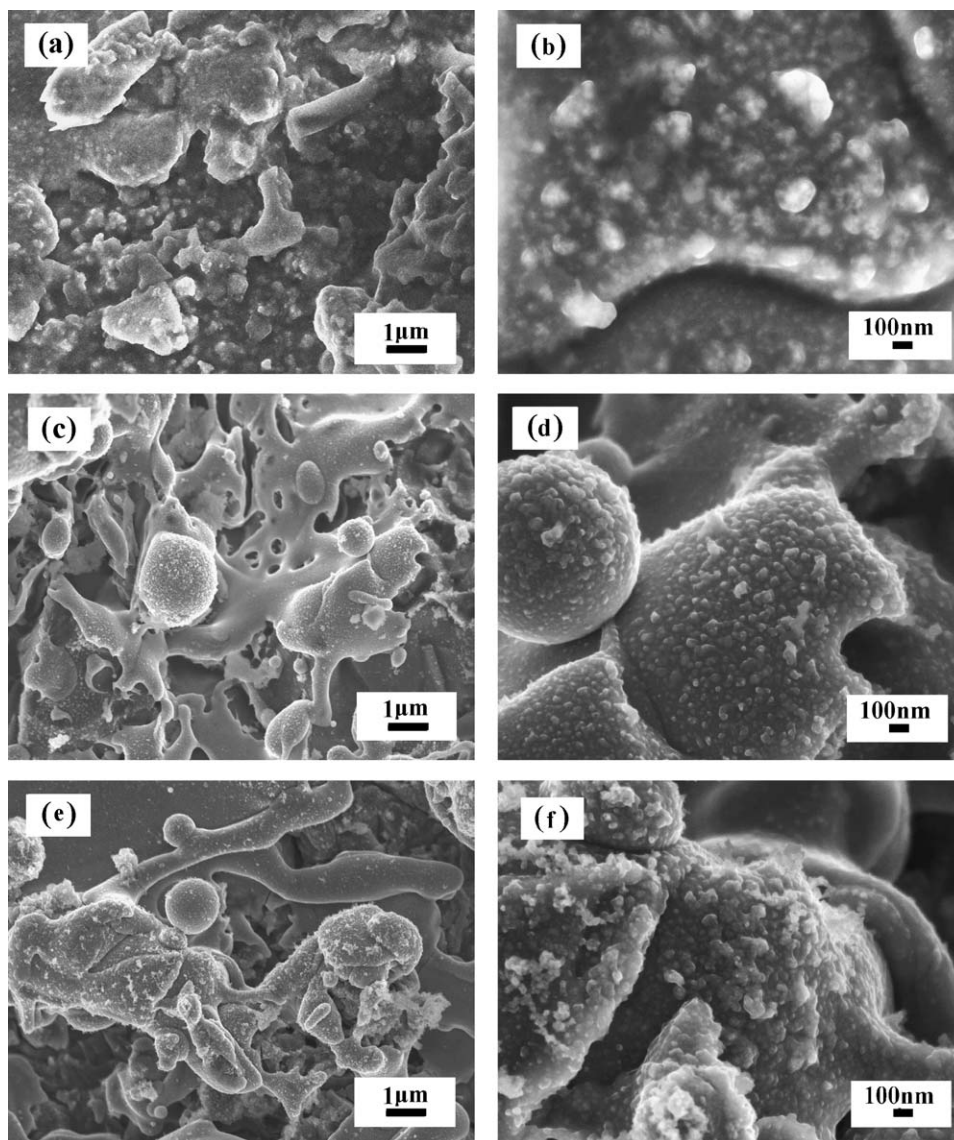


Fig. 7. The typical FESEM morphologies of plasma sprayed TiO_2 -based coatings: (a) and (b) 90% TiO_2 –10% ZnO ; (c) and (d) 90% TiO_2 –10% CeO_2 ; (e) and (f) 90% TiO_2 –10% SnO_2 .

seen from Fig. 8c. The mechanism for the splitting is not clear still.

Fig. 9a shows the evaluation of the $\text{Zn}2p$ spectra of the as-sprayed 90% TiO_2 –10% ZnO coating. The $\text{Zn}2p_{3/2}$ peak is observed at 1022.8 eV, exhibiting that Zn is only in oxide state. The intensity of Ce element on the surface of plasma sprayed 90% TiO_2 –10% CeO_2 coating is quite low as illustrated in Fig. 9b. The peak at 886.3 eV possibly corresponds to $\text{Ce}3d$ of CeO_2 . As shown in Fig. 9c, the $\text{Sn}3d$ spectrum recorded on the plasma sprayed 90% TiO_2 –10% SnO_2 coating shows two components associating with the $\text{Sn}3d_{5/2}$ at about 496.5 eV and $\text{Sn}3d_{3/2}$ at about 487.0 eV, which are in consistent with the reported values by C. Bittencourt.¹⁴ This suggests that the coating is mainly formed by Sn^{4+} species.

As can be seen from Fig. 10, the O1s of as-sprayed 90% TiO_2 –10% ZnO coating has a significant shift to lower

binding compared with the others. All the O1s XPS are asymmetric. The left side is wider than the right, indicating that three kinds of oxygen species presented in the surface or near-surface region by resolving their XPS curves. Peak 1 is connected with oxygen in the crystal lattice. Peak 2 is assigned to surface hydroxyl and peak 3 is due to physical-adsorbed oxygen. With the variation of additives ($\text{ZnO}/\text{CeO}_2/\text{SnO}_2$), the ratios among the three peaks are different. The as-sprayed 90% TiO_2 –10% SnO_2 coating exhibits the highest peak 2 and peak 3. In addition, the peak 2 is super than peak 1. In contrast, the plasma sprayed 90% TiO_2 –10% ZnO coating has the lowest peak in terms of surface hydroxyl. The surface hydroxyl group plays an important role in photocatalytic reaction. This will be discussed later in more detail combining with their photocatalytic activities of the three kinds of plasma sprayed TiO_2 -based coatings.

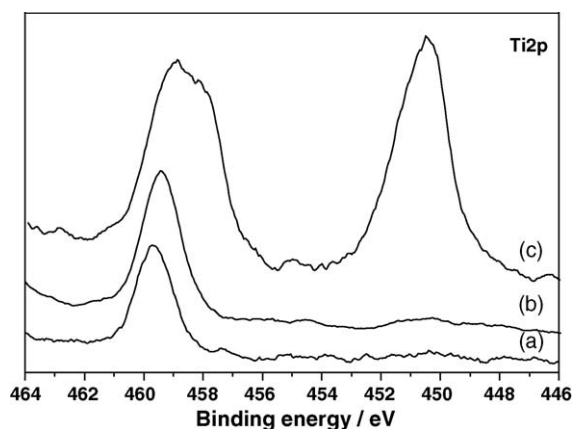


Fig. 8. The XPS of Ti2p on the surfaces of plasma sprayed TiO₂-based coatings: (a) 90%TiO₂–10%ZnO; (b) 90%TiO₂–10%CeO₂; and (c) 90%TiO₂–10%SnO₂.

3.2.4. Photocatalytic activity

Fig. 11 shows the dependence of benzene concentration on irradiation time using the three kinds of thin plasma sprayed TiO₂-based coatings as photocatalyst. It was noted that 11.8% reduction in benzene concentration was achieved at 10 h for the blank test, although there isn't any photocatalytic coating on the foamed aluminum plate. This result can be explained in terms of the absorption of the foamed aluminum plate resulting from its porous structure. At the first half hour, all the three kinds of plasma sprayed TiO₂-based coatings demonstrated fast decomposition rate due to their higher photocatalytic activity of the samples. With time went on, the surfaces of samples adsorbed the intermediates resulting from benzene decomposition which avoided the adsorption of benzene and then reduced the decomposition rate as can be seen from Fig. 11. The photocatalytic activity of plasma sprayed 90%TiO₂–10%ZnO coating was observed to be lower than the other two kinds of plasma sprayed TiO₂-based coatings. Approximate 91.6% of benzene was decomposed when used the plasma sprayed 90%TiO₂–10%ZnO coating as photocatalyst. The plasma sprayed 90%TiO₂–10%CeO₂ coating and 90%TiO₂–10%SnO₂ coating exhibited similar photocatalytic activity, they decomposed completely the benzene within 10 h as shown in Fig. 11.

It goes without saying that high anatase content is better to show high photocatalytic activity. Furthermore, it has been proved recently that the mixture of anatase and rutile phases has higher photocatalytic activity compared to pure anatase alone,^{15,16} although the real reason is not quite understood. In this study, all the three kinds of plasma sprayed TiO₂-based coatings present a mixture of anatase and rutile phases. The plasma sprayed 90%TiO₂–10%CeO₂ coating has the best photocatalytic activity in gas-phase benzene decomposition which is ascribed mainly to the highest anatase content as described above.

Surface morphology is also very important in photocatalytic activity. Prior to the photocatalytic reaction, the reactants must be adsorbed on the surface of photocatalyst. In

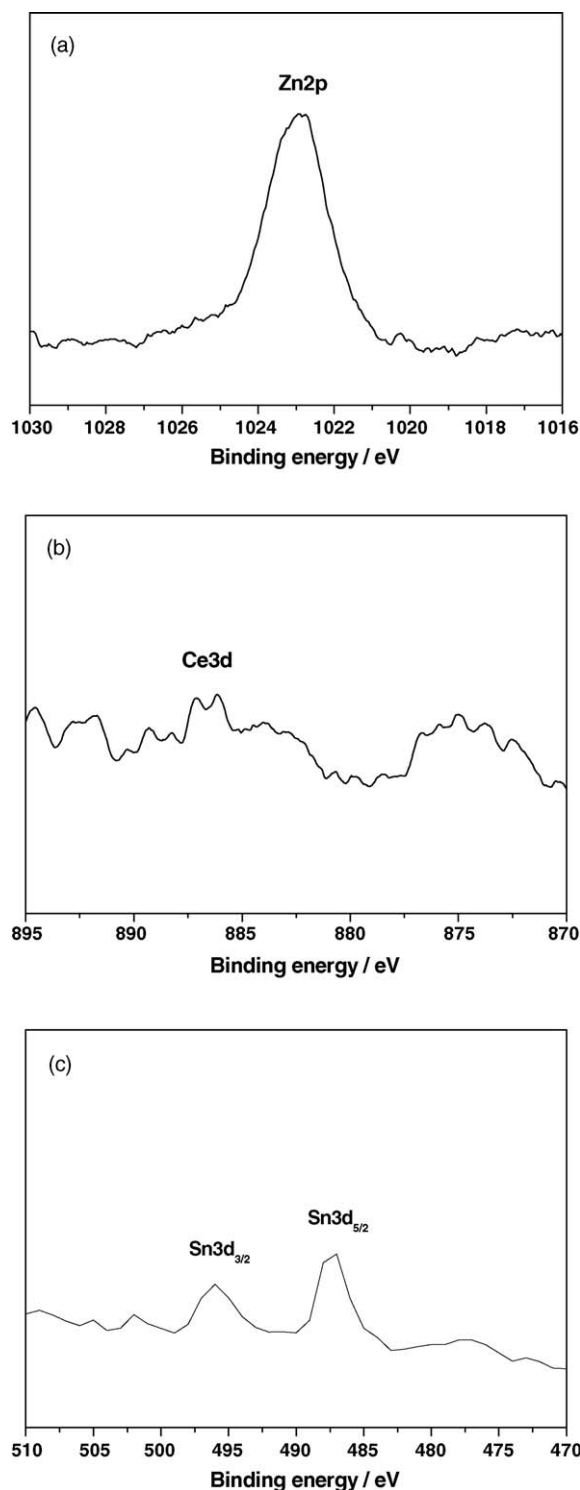


Fig. 9. (a) Zn2p, (b) Ce3d and (c) Sn3d XPS spectra of the plasma sprayed TiO₂-based coatings.

consequence, the photo-generated electron and hole transfer to the surface from inside, and then the photodecomposition takes place. As shown in Fig. 7d and f, the surfaces of plasma sprayed TiO₂-based coatings with additive of 10%CeO₂ and 10%SnO₂ are made of aggregated nanoparticles resembling

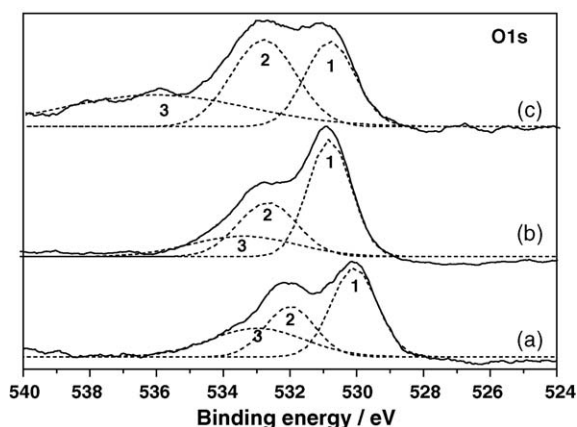


Fig. 10. The XPS of O1s on the surfaces of plasma sprayed TiO_2 -based coatings: (a) 90% TiO_2 –10% ZnO ; (b) 90% TiO_2 –10% CeO_2 ; and (c) 90% TiO_2 –10% SnO_2 .

the starting nano-particle, which could provide higher surface area and more active sites for the photocatalytic reaction. On the contrary, the plasma sprayed 90% TiO_2 –10% ZnO coating possesses larger particles on its surface as demonstrated in Fig. 7b. It is worth noticing, moreover, that the plasma sprayed 90% TiO_2 –10% SnO_2 coating has the highest content of surface hydroxyl (peak 2) as discussed above. The study by Pelizzetti showed that the surface photoactivity for a TiO_2 powder was proportional to the number of hydroxyl groups on its surface.¹⁷ The photogenerated holes can attack the surface hydroxyl and yield surface-bound hydroxyl radical ($\cdot\text{OH}$), which is an oxidizing agent and plays important roles in photocatalytic reaction.² With the increasing of surface hydroxyl content, the chance to form hydroxyl radical with photogenerated holes is increased. Correspondently, the transfer of photogenerated holes toward surface is accelerated resulting in improvement of photocatalytic activity. That is the reasons why the plasma sprayed TiO_2 coating with additive of 10% SnO_2 exhibited higher photocatalytic activity, although its anatase content is the lowest among the three

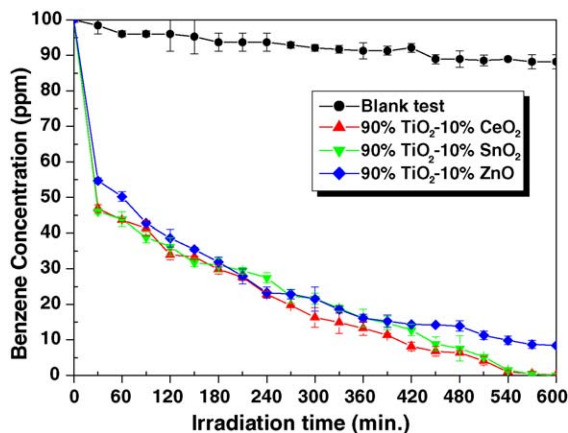


Fig. 11. The dependence of benzene concentration on irradiation time using the plasma sprayed TiO_2 -based coatings as photocatalyst.

TiO_2 -based coatings. Another possible reason for this behavior is that the conduction band of SnO_2 lies lower than those of TiO_2 and ZnO . Therefore, SnO_2 may act as a sink for removing photogenerated electrons from the TiO_2 and reducing electron–hole recombination.¹⁰

From these experimental results, it is concluded that the photocatalytic activity is not only dependent on the anatase content but also on the surface morphology and the hydroxyl content formed on the surface of plasma sprayed TiO_2 -based coatings as well as the additive character.

4. Conclusions

Using spray-dried composite powders as feedstock, three kinds of thin TiO_2 -based photocatalytic coatings were deposited on foamed aluminum by plasma spraying technique. The results showed that the plasma sprayed TiO_2 -based coatings were the mixture phases of anatase and rutile. The plasma sprayed TiO_2 -based coatings are characterized by nano-crystalline particles on the splats' surfaces. However, grain growth occurred on the surface of plasma sprayed 90% TiO_2 –10% ZnO coating. The XPS spectra revealed that the Ti, Zn, Ce and Sn elements existed on the surfaces of plasma sprayed TiO_2 -based coatings as the chemical states of Ti^{4+} , Zn^{2+} , Ce^{4+} and Sn^{4+} , respectively, whilst, the oxygen element was composed of three kinds of chemical states, i.e. crystal lattice oxygen, hydroxyl oxygen and physical-adsorbed oxygen. It was found that the plasma sprayed 90% TiO_2 –10% CeO_2 coating and 90% TiO_2 –10% SnO_2 coating exhibited similar photocatalytic activity. Both of them decomposed completely the gas-phase benzene within 10 h, while approximate 91.6% of benzene was decomposed when used the plasma sprayed 90% TiO_2 –10% ZnO coating as photocatalyst. It is concluded that the photocatalytic activity is not only dependent on the anatase content but also on the surface morphology and the hydroxyl content formed on the surface of plasma sprayed TiO_2 -based coatings as well as the additive character.

Acknowledgement

This study was supported by the Basic Research Program from the Korean Science and Engineering Foundation (KOSEF) under grant R01-2002-000-0035-0 (2002).

References

1. Fujishima, A. and Honda, K., Electrochemical photolysis of water at a semiconductor electrode. *Nature*, 1972, **238**, 37–38.
2. Fujishima, A., Rato, T. N. and Tryk, D. A., Titanium dioxide photocatalysis. *J Photochem Photobiol C: Photochem Rev*, 2000, **1**, 1–20.
3. Zeman, P. and Takabayashi, S., Nano-scaled photocatalytic TiO_2 thin films prepared by magnetron sputtering. *Thin Solid Films*, 2003, **1–2**, 57–62.

4. Bessekhoud, Y., Robert, D. and Weber, J. V., Synthesis of photocatalytic TiO_2 nanoparticles: optimization of the preparation conditions. *J Photochem Photobio A: Chem*, 2003, **157**, 47–53.
5. Jing, L. Q. X. J., Sun, X. J., Cai, W. M., Xu, Z. L., Du, Y. G. and Fu, H. G., The preparation and characterization of nanoparticle TiO_2/Ti films and their photocatalytic activity. *J Phys Chem Solids*, 2003, **64**, 615–623.
6. Bacsa, R. R. and Kiwi, J., Effect of rutile phase on the photocatalytic properties of nanocrystalline titania during the degradation of *p*-coumaric acid. *Appl Catal B: Environ*, 1998, **16**, 19–29.
7. Kandavelu, V., Kastien, H. and Thampi, K. R., Photocatalytic degradation of isothiazolin-3-ones in water and emulsion paints containing nanocrystalline TiO_2 and ZnO catalysts. *Appl Catal B: Environ*, 2004, **48**(2), 101–111.
8. Choi, W. Y., Termin, A. and Hoffmann, M. R., The role of metal dopants in quantum-sized TiO_2 : correlation between photo reactivity and charge carrier recombination dynamics. *J Phys Chem*, 1994, **98**, 13669–13679.
9. Do, Y. R., Lee, W., Dwyer, K. and Wold, A., The effect of WO_3 on the photocatalytic activity of TiO_2 . *J Solid State Chem*, 1994, **108**, 198–201.
10. Byrne, J. A., Eggins, B. R., Brown, N. M. D., McKinney, B. and Rouse, M., Immobilization of TiO_2 powder for the treatment of polluted water. *Appl Catal B: Environ*, 1998, **17**, 25–36.
11. Guillard, C., Beaugiraud, B., Dutriez, C., Hermann, J. M., Jaffrezic, H., Renault, N. J. et al., Physicochemical properties and photocatalytic activities of TiO_2 -films prepared by sol–gel methods. *Appl Catal B: Environ*, 2002, **39**, 331–342.
12. Chen, H., Zeng, Y. and Ding, C. X., Microstructural characterization of plasma-sprayed nanostructured zirconia powders and coatings. *J Eur Ceram Soc*, 2003, **23**, 491–497.
13. Gell, M., Jordan, E. H., Sohn, Y. H., Goberman, D., Shaw, L. and Xiao, T. D., Development and implementation of plasma sprayed nanostructured ceramic coatings. *Surf Coat Technol*, 2001, **146–147**, 48–54.
14. Bittencourt, C., Llobet, E., Ivanov, P., Correig, X., Vilanova, X., Brezmes, J. et al., Influence of the doping method on the sensitivity of Pt-doped screen-printed SnO_2 sensors. *Sens Actuators B: Chem*, 2004, **97**, 67–73.
15. Balasubramanian, G., Dionysiou, D. D., Suidan, M. T., Baudin, I. and Laine, J. M., Evaluating the activities of immobilized TiO_2 powder films for the photocatalytic degradation of organic contaminants in water. *Appl Catal B: Environ*, 2004, **47**, 73–84.
16. Zhang, Q. H., Gao, L. and Guo, J. K., Effect of calcination on the photocatalytic properties of nanosized TiO_2 powders prepared by TiCl_4 hydrolysis. *Appl Catal B: Environ*, 2000, **26**, 207–215.
17. Pelizzetti, E. and Minero, C., Mechanism of the photo-oxidative degradation of organic pollutants over TiO_2 particles. *Electrochim Acta*, 1993, **38**(1), 47–55.